Research & Reviews: Journal of Material Sciences
DOI: 10.4172/2321-6212.1000168

e-ISSN: 2321-6212
p-ISSN: 2347-2278

Hydrogen Storage in a Crosslinked Phloroglucinol-Terephthalaldehyde Framework with Exposed Iron Sites

Kapil Pareek[1], Rupesh Rohan[2] and Hansong Cheng[2,3]

[1]Centre for Energy and Environment, Malaviya National Institute of Technology, Jaipur, India

[2]Department of Chemistry, National University of Singapore, Singapore, 3 Science Drive 3, Singapore

[3]Sustainable Energy Laboratory, China University of Geoscience Whuan, 388 Lumo RD, Whuan, China

Research Article

Received: 10/05/2017
Accepted: 22/05/2017
Published: 29/05/2017

***For Correspondence**

Kapil Pareek, Centre for Energy and Environment, Malaviya National Institute of Technology, Jaipur, India, Tel: 0141-2713211.

Email: kapil.cee@mnit.ac.in

Keywords: Hydrogen storage, Physisorption, Heat of adsorption

ABSTRACT

Hydrogen adsorption has been studied in a cross-linked polymeric complex with coordinatively unsaturated iron metals. The complex displays hydrogen storage capacity up to 1.3 wt% at 298 K and 100 atm with an isosteric heat of adsorption up to 11.5 kJ mol^{-1}.

INTRODUCTION

The rapid consumption of fossil fuels worldwide has escalated greenhouse emission to a unsustainable level and has inspired the global research community to search for alternative energy resources [1]. Hydrogen is an environmentally clean and efficient energy carrier for a wide variety of applications [2]. Unfortunately, lack of safe, high density hydrogen storage methods at near ambient conditions has been deemed to be the bottleneck that prevents broad market acceptance of hydrogen technologies. Technically, hydrogen storage can be realized via chemisorption [3] in the form of chemical hydrides [4], complex hydrides [3], or physisorption [1] in porous carbon based materials [5], zeolites [6], metal organic frameworks (MOFs) [1,7,8] and porous organic frameworks (POFs) [9-15]. Nevertheless, most of the chemisorption-based materials exhibit relatively poor kinetics and require an elevated temperature to release the hydrogen gas [3], while most of the physisorption-based materials show fast adsorption-desorption kinetics but negligible hydrogen storage capacity at ambient temperature due to the weak host-H_2 interaction in the range of 3-7 kJ mol^{-1} [16]. It has been shown that hydrogen storage capacity in physisorption-based materials can be improved if the associated enthalpy of adsorption is enhanced in the range of 15-20 kJ mol^{-1}, which is substantially higher than the typical van der Waals force [17].

To enhance H_2 affinity in a host material via physisorption, extensive research efforts have been made to develop materials with coordinatively unsaturated metal sites. The metal elements selected are chiefly from the first row of transition metal series due to their unique capabilities to stabilize the M-η^2-H_2 complexes via electron backdonation from metal d-orbitals to the antibonding orbital of H_2 (σ^*) and to accommodate several H_2 molecules per each metal atom [18,19]. For example, in a phloroglucinol-terephthalaldehyde based framework with coordinatively unsaturated Cr metals, a high excess hydrogen uptake up to 1.5 wt% at 298 K and 100 atm with an isosteric heat of adsorption (Qst) up to 11.5 kJ mol^{-1} has been reported recently by our group [18]. Sumida et al. [20] also demonstrated a high Qst of 11.9 kJ mol^{-1} on coordinatively unsaturated iron metal sites in Fe-BTT MOF (BTT^{3-}=1,3,5-benzenetristetrazolate). Similar observations have also been made in several recent studies [21,22].

In this work, we report hydrogen storage with a significant capacity in a mesoporous phloroglucinol-terephthalaldehyde framework compound decorated with exposed iron atoms (PTF-Fe) [23]. Detailed characterizations of the PTF-Fe complex

Research & Reviews: Journal of Material Sciences
DOI: 10.4172/2321-6212.1000168
e-ISSN: 2321-6212
p-ISSN: 2347-2278

and comparison of adsorption properties with contemporary storage materials with coordinatively unsaturated metal sites have been presented to provide better understanding of hydrogen storage on exposed metals sites.

Synthesis of PTF-Fe complex

PTF-Fe was synthesized in a three-step reaction, as shown in **Scheme 1**. In the first step, synthesis of $Fe[N(SiMe_3)_2]_2$ was done by reacting $FeCl_2$ with 2 molar equivalent of $LiN(SiMe_3)_2$ at room temperature in an anhydrous tetrahydrofuran solvent under argon atmosphere followed by purification, similar to the published procedure [24-29]. In the second step, a flame-dried three neck flask fitted with a magnetic stirring bar was charged with phloroglucinol (500 mg, 3.96 mmol) and toluene (40 ml) solvent. After degassing by argon bubbling, $Fe[N(SiMe_3)_2]_2$ (5.94 mmol) was charged to the above flask and heated at 80°C for 12 hrs under argon atmosphere which produced the Fe-modified-phloroglucinol and hexamethyldisilazane (HMDS) [27,28]. The solvent and HMDS was removed under reduced pressure. In the third step, Fe-modified-phloroglucinol, terephthaldehyde (796 mg, 5.94 mmol) and 15 ml 1,4 dioxane were charged into a Teflon lined autoclave in a glove box. The autoclave was placed in an oven at 180°C for 4 days. After cooling at room temperature, the PTF-Fe was washed with excess of THF, 1,4 dioxane and hexane. The PTF-Fe was dried in a tube furnace at 180°C for 24 hrs to produce a red color solid with a yield of 86%. Elemental analysis: calculated theoretically C 50.71, H 1.86, Fe 22.10 found (CHNS and ICP-MS): C 44.18, H 2.75, Fe 18.11.

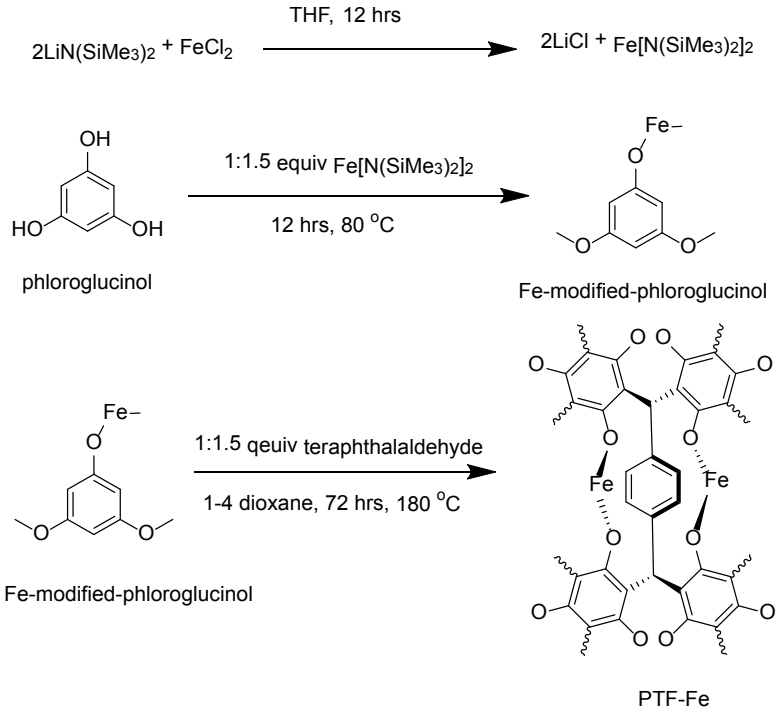

Scheme 1. Synthesis protocol of PTF-Fe complex.

Characterizations

Powder X-ray diffraction (XRD) was performed on a D5005 Bruker AXS diffractometer with Cu-Kα radiation (λ=1.5410 A°) at room temperature. A sample size of 70-110 mg was used for the XRD measurement. SEM images were obtained using a scanning electron microscopy (SEM) with Jeol JSM-6701F. Samples were prepared by gold sputtering under 9Pa at room temperature (20 s, 30 mA) with a JEOL JFC 1600 Fine Coater. All X-ray photoelectron spectra (XPS) were taken with a Kratos AXIS Ultra^{DLD} spectrometer. Infrared spectroscopy was taken on the Varian resolutions (version 4.0.5.009). Thermogravimetric analysis was performed on a TA instrument 2960 (DTA-TGA) at the heating rate of 5°C min^{-1}. Nitrogen gas adsorption-desorption isotherms were performed using a Micromeritics ASAP 2020 instrument. High pressure hydrogen uptake measurements were obtained on a computer-controlled commercial Gas Reaction Controller (GRC) manufactured by Advanced Materials Corporation. Hydrogen adsorption measurements were performed by following the standard practice guidelines provided by the US Department of Energy to minimize potential errors in the hydrogen uptake measurement [30-32]. The instrument calibration and the experimental considerations are published elsewhere [11-13,15,18].

Enthalpies of adsorption were derived from the following eqn. (1):

$$\left[\frac{\partial \ln p}{\partial\left(\frac{1}{T}\right)_\theta}\right] = \frac{\Delta_{ad}H}{R} \quad (1)$$

Where T represents the temperature, p is the pressure (in kPa), $\Delta_{ad}H$ is the enthalpy of adsorption and R is the universal gas constant [1]. A plot of ln*p* against 1/T is a straight line of the slope $\Delta_{ad}H/R$ at a given surface coverage.

Research & Reviews: Journal of Material Sciences
DOI: 10.4172/2321-6212.1000168
e-ISSN: 2321-6212
p-ISSN: 2347-2278

RESULTS AND DISCUSSIONS

The PTF-Fe complex exhibits poor solubility in common organic solvents and displays higher thermal stability than monomers **(Figure 1a)**. The initial 10% weight loss before 200°C is attributed to a loss of solvent molecules and moisture trapped inside the pores of the compound and a steep weight loss around 410°C under nitrogen environment is attributed to the decomposition of the framework. In the FTIR spectrum of PTF-Fe, **(Figure 1b)** the characteristic bands of the –CHO functional groups (2870 cm^{-1}, C-H str.; 1690 cm^{-1}, C=O str.) and phloroglucinol (1188 cm^{-1} and 1008 cm^{-1}) are weaker than in the monomers, consistent with the expected polymer structure [11,33].

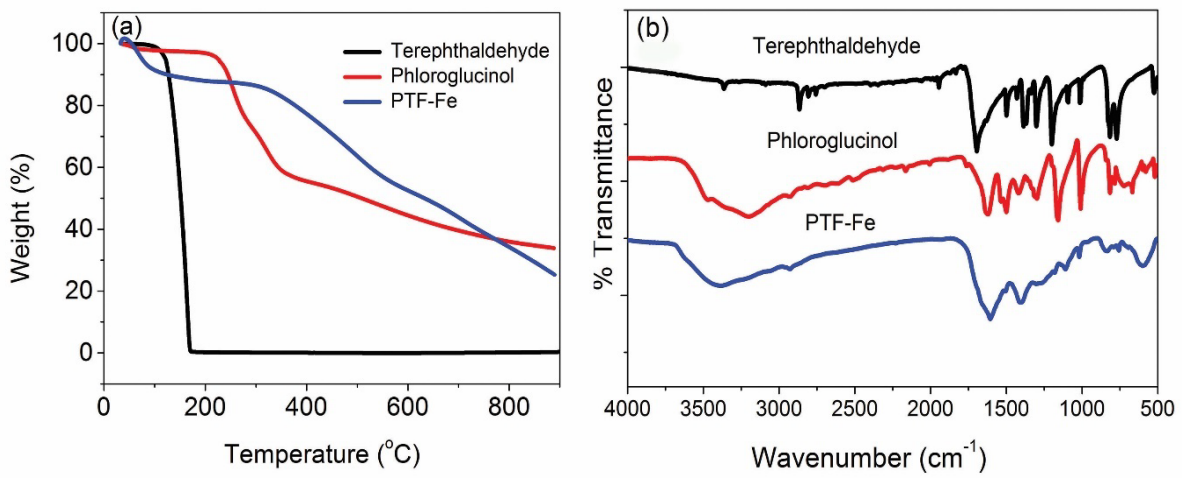

Figure 1. (a) TGA thermograms of terephthalaldehyde, phloroglucinol, and PTF-Fe under N_2 atmosphere, and (b) FTIR spectra of terephthalaldehyde, phloroglucinol, and PTF-Fe.

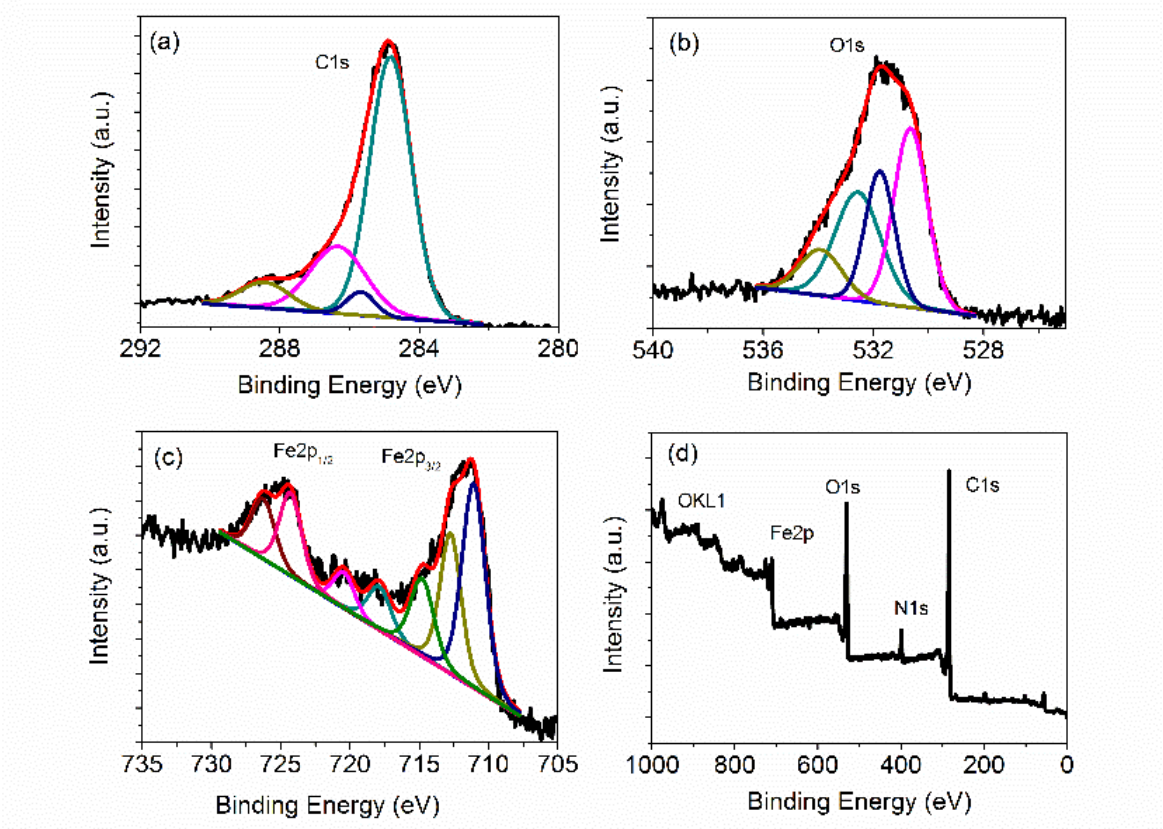

Figure 2. X-ray photoelectron (XPS) spectra (a) high resolution scan of C 1s, (b) high resolution scan of O 1s, (c) high resolution scan of Fe $2p_{1/2}$ and $2p_{3/2}$, and (d) a complete scan for PTF-Fe.

The deconvoluted X-ray photoelectron spectra (XPS) of PTF-Fe complex is displayed in **Figure 2**. A binding energy of 531.72 eV for the O1s orbital indicates that oxygen is coordinated with an iron atom **(Figure 2b)** [34,35]. The binding energies of the Fe $2p_{3/2}$ and Fe $2p_{1/2}$ peaks are up to 711.41 eV and 724.74 eV, respectively **(Figure 2c)**, which arise from the high electronegativity of the coordinated oxygen atoms of the framework compound [36].

Research & Reviews: Journal of Material Sciences
DOI: 10.4172/2321-6212.1000168
e-ISSN: 2321-6212
p-ISSN: 2347-2278

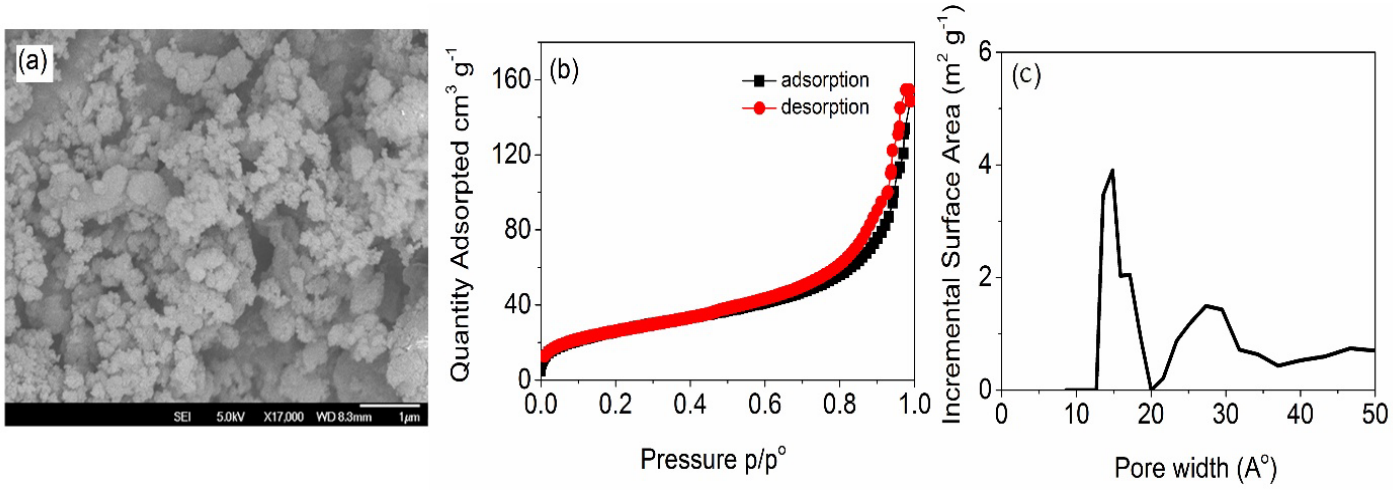

Figure 3. (a) SEM micrograph of PTF-Fe complex, (b) Nitrogen adsorption-desorption isotherms at 77 K and 1 bar, and (c) pore size distribution calculated from the nitrogen adsorption-desorption isotherms at 77 K by applying the DFT pore size analysis method for PTF-Fe complex.

The surface morphology of the PTF-Fe complex was investigated using scanning electron microscopy (SEM) **(Figure 3a)**. The PTF-Fe complex was found to have a series of loosely packed interconnected agglomerates. The specific surface area and the pore size distribution of the PTF-Fe complex were analyzed based on the nitrogen gas adsorption-desorption isotherms at 77 K and 1 atm pressure **(Figure 3b and 3c)**. The PTF-Fe complex exhibits a Type IV adsorption isotherm [37] with a small desorption hysteresis, confirming the mesoporous nature of the material. The complex has a Brunauer–Emmett–Teller (BET) surface area up to 106 $m^2 g^{-1}$, significantly lower than the surface areas of most MOFs, activated carbons but comparable to the value of metal hydrazide gel materials (90-550 $m^2 g^{-1}$) [1,38-40]. The Density Functional Theory (DFT) pore size distributions of the PTF-Fe complex derived using the entire range of the N_2 adsorption isotherms confirm that the size of the majority of pores is about 1.5 nm, which is beneficial for H_2 gas adsorption due to the strong host-H_2 interaction originated from the overlap of the pore wall potentials **(Figure 3c)** [41].

Most adsorbents display a “Type I” isotherm upon physisorption of molecular hydrogen on surfaces at 77 K and low pressure (up to 1 atm). At a high pressure (usually within 100 atm), the isotherm shows a saturation capacity reflected as the “knee point”, beyond which the excess capacity decreases with pressure [1]. Interestingly, at 298 K and a pressure within 100 atm, these materials show a straight adsorption line due to the weak host-H_2 interaction. On the other hand, the Kubas type metal hydrazide gel materials [19] show a straight adsorption line both at 77 K and 298 K within pressures of 100 atm suggesting different adsorption behaviour with relatively stronger host-H_2 interaction [38-40]. Similarly, the PTF-Fe complex exhibits a straight adsorption line both at 77 K and 298 K **(Figure 4a and 4b)**. Notably, the apparatus with an empty sample chamber was thoroughly calibrated prior to the test to rule out a linear increase of uptake upon gas compression. The instrument calibration and the experimental considerations are published elsewhere [11-13,15,18].

The isotherm at 77 K confirms a maximum excess hydrogen storage capacity of 1.65 wt% at 100 atm for PTF-Fe, substantially lower than the capacities of high surface area porous materials [1] but comparable to the values of Kubas type gel materials [38,39,42,43]. At 298 K and 100 atm, the PTF-Fe shows an excess hydrogen storage capacity of 1.3 wt%, higher than the uptake of many MOFs with exposed metal sites [1,7,8]. It should be noted that the hydrogen storage capacity of the PTF-Fe is comparable to that of the Kubas type gel materials even in 4 folds lower metal loading (18% vs 50-80%), which is attributed to the relatively higher exposure of the cations in PTF-Fe. Notably, there is a large hysteresis observed between the adsorption and desorption isotherms in low pressure (up to 1 atm) at 77 K, rarely observed in other physisorption-based materials and might be caused by the strong adsorption of H_2 on exposed iron cations in the complex **(Figure 4b)**. The adsorption was found to be completely reversible with stable cycle performance at 298 K and 100 atm as demonstrated in **Figure 4c**.

Research & Reviews: Journal of Material Sciences
DOI: 10.4172/2321-6212.1000168
e-ISSN: 2321-6212
p-ISSN: 2347-2278

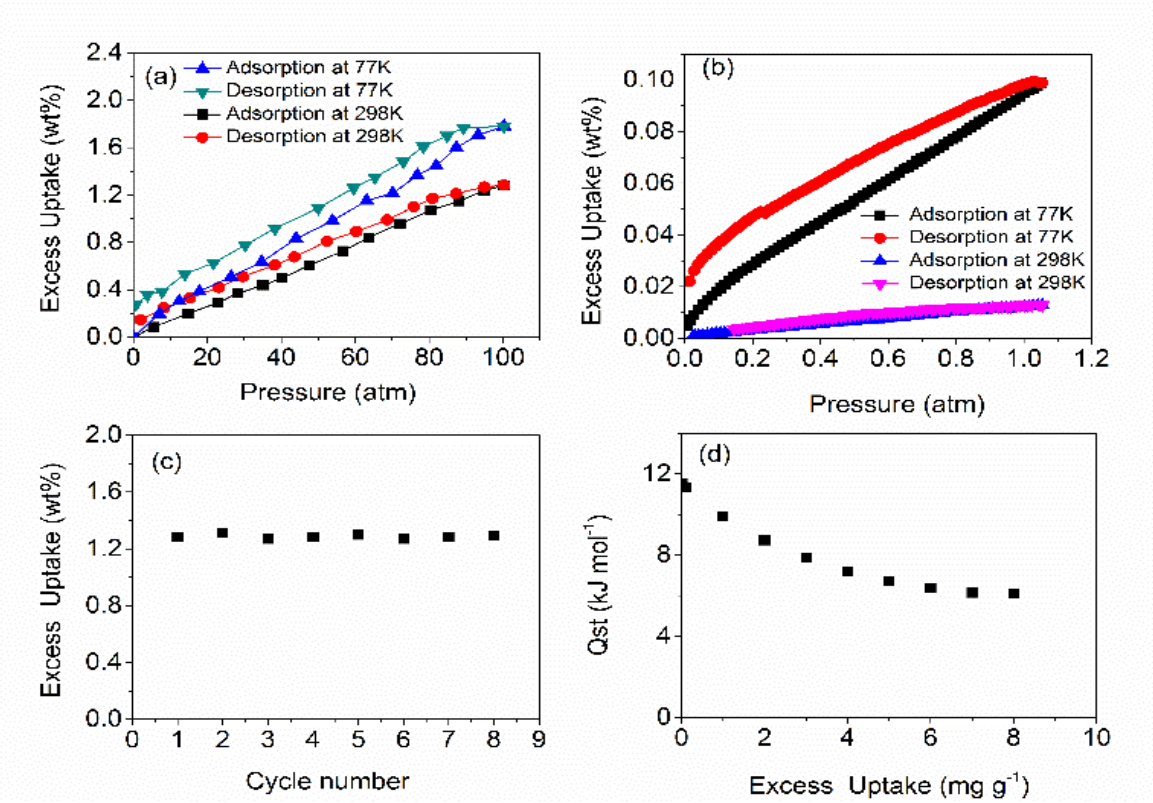

Figure 4. In PTF-Fe complex (a) high pressure excess hydrogen uptake at 298 K and 77 K, (b) low pressure excess hydrogen uptake at 298 K and 77 K, (c) hydrogen excess capacity at 298 K in eight fully reversible adsorption-desorption cycles up to 100 atm, and (d) calculated isosteric heat of adsorption.

To quantitatively describe the interaction, the isosteric heat of adsorption (Qst) was derived from the measured isotherms at 298 K and 323 K using the Virial method **(Figure 4d)**. The zero coverage Qst was found up to 11.5 kJ mol^{-1}, higher than the reported value for most of MOFs with open metal sites [1]. The strong interaction between hydrogen and the host material is consistent with the observed high hydrogen uptake, which can be understood based on the nature of bonding. According to Kubas [44], the H_2 molecule acts as a weak Lewis base which can bind strongly to a metal centre as a nonbonding pair, and the resulting M-||^2-H_2 complex with a side-on configuration can be stabilized via the back-donation of electrons from a filled metal d orbital to the antibonding orbital of H_2 (σ*).

Table 1. A comparison of excess hydrogen uptake capacities, BET surface areas and heats of hydrogen adsorption of some reported MOF materials with PTF-Fe of present work.

Entry	S_{BET} (m^2g^{-1})	Excess Uptake (wt%)	Qst (kJ mol^{-1})	Pressure (atm)	Reference
1	905	0.26	6.65	70	SNU-21S [45]
2	3000	0.66	6.36	90	PCN-61 [46]
3	4000	0.78	6.22	90	PCN-66 [46]
4	5109	1.02	6.09	90	PCN-68 [46]
5	2100	0.94	10.10	90	Mn-BTT [47]
6	1710	0.46	9.50	90	Cu-BTT [48]
7	1510	0.42	10.30	100	MOF-74 [49]
8	2300	0.39	7.10	100	SNU-50 [50]
9	2010	0.50	11.90	100	Fe-BTT [20]
10	106	1.50	11.50	100	[a]PTF-Cr [18]
11	128	0.50	8.00	100	[a]PTF-Mg [18]
12	175	1.70	14.8	100	[a]MTF-Fe [12]
13	137	0.80	12.00	100	[a]MTF-Mg [15]
14	106	1.30	11.50	100	*PTF-Fe

*Present Work, [a]Previously reported by the same group.

The comparison between PTF-Fe and a set of H_2 physisorption MOFs with the exposed metal sites is tabulated in **Table 1**. Evidently, the PTF-Fe complex displays a higher Qst value than these MOFs [1]. This is attributed to the higher degree of exposure of the metal sites to molecular hydrogen. In particular, we note that among the materials listed

e-ISSN: 2321-6212
p-ISSN: 2347-2278

in **Table 1**, the surface area of the PTF-Fe complex is significantly lower but the gravimetric hydrogen uptake of the compound is high. The oxygen linkers provide strong chelation to stabilize the coordinatively unsaturated iron atoms in the PTF-Fe complex. Unfortunately, the relatively low surface area of the PTF-Fe complex may lead to low exposure of the iron cations to store molecular hydrogen with even higher capacity at room temperature. Nevertheless, this experiment represents an important direction for search of better materials for hydrogen storage via physisorption [45-50].

CONCLUSION

A facile synthesis of a cross-linked organo-iron complex with highly exposed iron metal sites was presented for room temperature hydrogen storage via physisorption. The synthesized PTF-Fe complex exhibits a moderate BET specific surface area of 106 $m^2 g^{-1}$ and an excess hydrogen uptake of 1.30 wt% at 298 K and 100 atm, higher than most of the MOFs with coordinatively unsaturated metal sites but comparable to the Kubas type gel materials. The high hydrogen uptake arises from the strong sorbent-sorbate interaction, supported by the low coverage isosteric heat of adsorption of 11.5 kJ mol^{-1}, which is higher than the reported values of most MOFs. Nevertheless, the moderate surface area prevents a complete exposure of the Fe cations in the PTF-Fe complex to molecular hydrogen to achieve a higher storage capacity. One possible avenue for the future work is to improve specific surface area of the material with more exposed metal sites to further enhance both enthalpy of adsorption and hydrogen uptake capacity at 298 K, which is planned in our future work.

REFERENCES

1. Suh MP, et al. Hydrogen Storage in Metal–Organic Frameworks. Chem Rev 2011;112:782-835.
2. http://www.hydrogen.energy.gov/storage.html
3. Orimo Si, et al. Complex Hydrides for Hydrogen Storage. Chem Rev 2007;107:4111-4132.
4. Biniwale RB, et al. Chemical hydrides: A solution to high capacity hydrogen storage and supply. Int J Hydrogen Energ 2008;33:360-365.
5. Yürüm Y, et al. Storage of hydrogen in nanostructured carbon materials. Int J Hydrogen Energ 2009;34:3784-3798.
6. Langmi HW, et al. Hydrogen storage in ion-exchanged zeolites. J Alloys Comp 2005;404-406:637-642.
7. Dincă M and Long JR. Hydrogen Storage in Microporous Metal–Organic Frameworks with Exposed Metal Sites. Angewandte Chemie Int Edn 2008;47:6766-6779.
8. Vitillo JG, et al. Role of Exposed Metal Sites in Hydrogen Storage in MOFs. J Am Chem Soc 2008;130:8386-8396.
9. Xiang Z and Cao D. Porous covalent-organic materials: synthesis, clean energy application and design. J Mater Chem A 2013;1:2691-2718.
10. Dalebrook AF, et al. Hydrogen storage: beyond conventional methods. Chem Commun 2013;49:8735-8751.
11. Pareek K, et al. Highly selective carbon dioxide adsorption on exposed magnesium metals in a cross-linked organo-magnesium complex. J Mater Chem A 2014;2:13534-13540.
12. Pareek K, et al. Room Temperature Hydrogen Physisorption on Exposed Metals in a Highly Cross-Linked Organo-Iron Complex. Adv Mater Interf 2014.
13. Pareek K, et al. Hydrogen physisorption in ionic solid compounds with exposed metal cations at room temperature. RSC Adv 2014;4:33905-33910.
14. Xu G, et al. High capacity hydrogen storage at room temperature via physisorption in a coordinatively unsaturated iron complex. Int J Hydrogen Energ 2015;40:16330-16337.
15. Pareek K, et al. Polymeric organo-magnesium complex for room temperature hydrogen physisorption. RSC Adv 2015;5:10886-10891.
16. Zhao D, et al. The current status of hydrogen storage in metal-organic frameworks. Energ Environ Sci 2008;1:222-235.
17. Bhatia SK and Myers AL. Optimum Conditions for Adsorptive Storage. Langmuir 2006;22:1688-1700.
18. Pareek K, et al. Ambient temperature hydrogen storage in porous materials with exposed metal sites. Int J Hydrogen Energ 2017;42:6801-6809.
19. Skipper CVJ, et al. Are Metal–Metal Interactions Involved in the Rising Enthalpies Observed in The Kubas Binding of H_2 to Hydrazine-Linked Hydrogen Storage Materials? J Phys Chem C 2012;116:19134-19144.
20. Sumida K, et al. Hydrogen storage and carbon dioxide capture in an iron-based sodalite-type metal-organic framework (Fe-BTT) discovered via high-throughput methods. Chem Sci 2010;1:184-191.

e-ISSN: 2321-6212
p-ISSN: 2347-2278

21. Oh H, et al. Efficient synthesis for large-scale production and characterization for hydrogen storage of ligand exchanged MOF-74/174/184-M (M=Mg^{2+}, Ni^{2+}). Int J Hydrogen Energ 2017;42:1027-1035.

22. Gohari-Bajestani Z, et al. Synthesis of anatase TiO_2 with exposed (001) facets grown on N-doped reduced graphene oxide for enhanced hydrogen storage. Int J Hydrogen Energ 2017;42:6096-6103.

23. Katsoulidis AP and Kanatzidis MG. Phloroglucinol Based Microporous Polymeric Organic Frameworks with −OH Functional Groups and High CO_2 Capture Capacity. Chem Mater 2011;23:1818-1824.

24. Andersen RA, et al. Synthesis of bis[bis(trimethylsilyl)amido]iron(II). Structure and bonding in M[N(SiMe3)2]2 (M=manganese, iron, cobalt): two-coordinate transition-metal amides. Inorg Chem 1988;27:1782-1786.

25. Bradley DC and Chisholm MH. Transition-metal dialkylamides and disilylamides. Accounts Chem Res 1976;9:273-280.

26. Bradley DC, et al. Transition Metal Complexes of Bis(Trimethyl-silyl)Amine (1,1,1,3,3,3-Hexamethyldisilazane), in Inorganic Syntheses. John Wiley & Sons Inc. 2007;112-120.

27. Horvath B and Horvath EG. Chromium (II) Alkoxides. Zeitschrift für anorganische und allgemeine Chemie 1979;457:51-61.

28. Horvath B, et al. Chromium (II) Silylamides. Zeitschrift für anorganische und allgemeine Chemie, 1979;457:38-50.

29. Rohan R, et al. A pre-lithiated phloroglucinol based 3D porous framework as a single ion conducting electrolyte for lithium ion batteries. RSC Adv 2016;6:53140-53147.

30. Broom DP. The accuracy of hydrogen sorption measurements on potential storage materials. Int J Hydrogen Energ 2007;32:4871-4888.

31. Broom DP. Accuracy in hydrogen sorption measurements. J Alloys Comp 2007;446-447:87-691.

32. Broom DP. Hydrogen sorption measurements on potential storage materials: experimental methods and measurement accuracy. EUR 23242 EN. Office for Official Publications of the European Communities, Luxembourg 2008.

33. Rohan R, et al. Melamine-terephthalaldehyde-lithium complex: a porous organic network based single ion electrolyte for lithium ion batteries. J Mater Chem A 2015;3:5132-5139.

34. Biesinger MC, et al. Resolving surface chemical states in XPS analysis of first row transition metals, oxides and hydroxides: Cr, Mn, Fe, Co and Ni. Appl Surf Sci 2011;257:2717-2730.

35. Haber J, et al. X-ray photoelectron spectra of oxygen in oxides of Co, Ni, Fe and Zn. J Electron Spectrosc Relat Phenomena 1976;9:459-467.

36. Seah MP. The quantitative analysis of surfaces by XPS: A review. Surf Interf Anal 1980;2:222-239.

37. Schneider P. Adsorption isotherms of microporous-mesoporous solids revisited. Appl Cataly A: Gen 1995;129:157-165.

38. Hoang TKA, et al. Multivalent Manganese Hydrazide Gels for Kubas-Type Hydrogen Storage. Chem Mater 2012;24:1629-1638.

39. Hamaed A, et al. Hydride-Induced Amplification of Performance and Binding Enthalpies in Chromium Hydrazide Gels for Kubas-Type Hydrogen Storage. J Am Chem Soc 2011;133:15434-15443.

40. Mai HV, et al. Cyclopentadienyl chromium hydrazide gels for Kubas-type hydrogen storage. Chem Commun 2010;46:3206-3208.

41. Lowell SS, et al. Characterization of Porous Solids and Powders: Surface Area, Pore Size and Density. Springer 2004.

42. Skipper CVJ, et al. The Kubas interaction in M(ii) (M=Ti, V, Cr) hydrazine-based hydrogen storage materials: a DFT study. Dalton Trans 2012;41:8515-8523.

43. Hoang TKA, et al. Kubas-Type Hydrogen Storage in V(III) Polymers Using Tri- and Tetradentate Bridging Ligands. J Am Chem Soc 2011;133:4955-4964.

44. Kubas GJ. Fundamentals of H_2 Binding and Reactivity on Transition Metals Underlying Hydrogenase Function and H_2 Production and Storage. Chem Rev 2007;107:4152-4205.

45. Kim TK and Suh MP. Selective CO_2 adsorption in a flexible non-interpenetrated metal-organic framework. Chem Commun 2011;47:4258-4260.

46. Yuan D, et al. An Isoreticular Series of Metal–Organic Frameworks with Dendritic Hexacarboxylate Ligands and Exceptionally High Gas-Uptake Capacity. Angewandte Chemie Int Edn, 2010;49:5357-5361.

47. Dinca M, et al. Hydrogen Storage in a Microporous Metal−Organic Framework with Exposed Mn^{2+} Coordination Sites. J Am Chem Soc 2006;128:16876-16883.

48. Dincă M, et al. Observation of Cu^{2+}–H_2 Interactions in a Fully Desolvated Sodalite-Type Metal–Organic Framework. Angewandte Chemie Int Edn, 2007;46:1419-1422.

e-ISSN: 2321-6212
p-ISSN: 2347-2278

49. Sumida K, et al. Hydrogen storage properties and neutron scattering studies of Mg2(dobdc)-a metal-organic framework with open Mg^{2+} adsorption sites. Chem Commun 2011;47:1157-1159.

50. Prasad TK, et al. High Gas Sorption and Metal-Ion Exchange of Microporous Metal–Organic Frameworks with Incorporated Imide Groups. Chem–Euro J 2010;16:14043-14050.